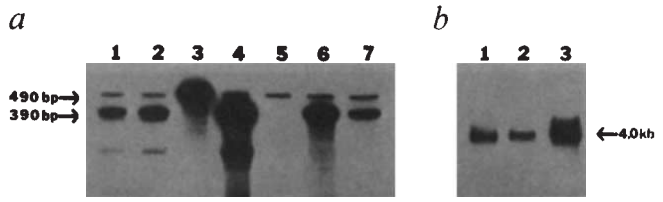

Fig. 3 Expression of *GLI* in Tera 1 and Tera 2 cells. *a*, RNase A protection analysis using a 490 bp probe that contains 390 bp of *GLI* zinc finger sequence flanked by vector. Lane 1, Tera-1 cell RNA (25 μg); lane 2, NTera-2 cell RNA (25 μg); lane 3, probe alone (not subjected to RNase A treatment); lane 4, D-259 MG cell RNA (9 μg); lane 5, yeast tRNA (25 μg); lane 6, 150 pg of *in vitro* transcribed 3,600 bp *GLI* transcript corresponding to ~30 copies per cell; lane 7, 30 pg of *in vitro* transcribed 3,600 bp GLI transcript corresponding to ~6 copies per cell. *b*, Northern blot analysis using λJ36 as probe. Lanes were loaded with poly(A^+) RNA isolated from: Lane 1, Tera-1 cells; lane 2, NTera-2 cells; lane 3, D-259 MG cells.

Methods. Tera-1 cells[26] were from the American Type Culture Collection, NTera-2 cells[27] were provided by P. Andrews. Total RNA was isolated by the acid guanidium isothiocyanate–phenol–chloroform extraction method[28]. The ^{32}P labelled RNA probe for RNase A protection was a sublcone of λI2G containing the last four zinc fingers of GLI (nucleotides 796–1189) cloned in Bluescript. RNase A protection was performed as described[29] but with the following modifications: hybridizations were in a final volume of 10 μl; only RNase A (12.5 μg ml^{-1}) was used; and the RNase A and Proteinase K incubations were at room temperature for 30 min. Calculations of copy number per cell were based on a total RNA content of 10 pg per cell. For Northern analysis poly(A^+) RNA was isolated from 50 μg total RNA (Tera-1 and NTera-2) or 22 μg total RNA (D-259 MG) by selection on oligo-dT cellulose, separated by electrophoresis through a 1.5% MOPS/formaldehyde gel and transferred in dilute alkali to nylon (Bio-Rad) using conditions recommended by the supplier. The insert from a λJ36 subclone was labelled with ^{32}P by the random primer method[20] and hybridized to the filter at 50 °C in 50% formamide, 2 × SSPE, 7% SDS, 0.5% nonfat dried milk, 0.2 mg ml^{-1} salmon sperm DNA (10 × SSPE = 1.8 M NaCl, 100 mM $NaPO_4$, 10 mM EDTA, *p*H 7.0). Band sizes were determined by comparison to migration of an RNA standard ladder (BRL). The previously reported size (4.8 kb, ref. 2) for the *GLI* transcript in D-259 MG cells was the result of the slower migration of transcripts in lanes containing total RNA.

National Cancer Institute training grants CA-09243 (K.W.K.) and GM-07184 (J.M.R.) and NIH grants CA-43722 (S.H.B.), NS-20023 (S.H.B.), and CA-43460(B.V.).

Received 5 January; accepted 4 February 1988.

1. Bishop, J. M. *Science* **235,** 305-311 (1987).
2. Kinzler, K. W. *et al. Science* **236,** 70-73 (1987).
3. Wong, A. J. *et al. Proc. natn. Acad. Sci. U.S.A.* **84,** 6899-6903 (1987).
4. Miller, J., McLachlan, A. D & Klug, A. *EMBO J.* **4,** 1609-1614 (1985).
5. Schuh, R. *et al. Cell* **47,** 1025-1032 (1986).
6. Chowdhury, K., Deutsch, U. & Gruss, P. *Cell* **48,** 771-778 (1987).
7. Bigner, S. H., Mark, J. & Bigner, D. D. *Cancer Genet. Cytogenet.* **24,** 163-176 (1987).
8. Kozak, M. *Nucleic Acids Res.* **15,** 8125-8133 (1987).
9. Berg, J. M. *Science* **232,** 485-487 (1986).
10. Preiss, A., Rosenberg, U. B., Kienlin, A., Seifert, E. & Jackle, H. *Nature* **315,** 27-32 (1985).
11. Rosenberg, U. B. *et al. Nature* **319,** 336-339 (1986).
12. Huganir, H. L. in *Neuromodulation: The Biochemical Control of Neuronal Excitability* (eds Kaczmarek, L. K. & Levitan, I. B.) 64-85 (Oxford University Press, New York, 1987).
13. Shapiro, M. B. & Senapathy, P. *Nucleic Acids Res.* **15,** 7155-7174 (1987).
14. Bohmann, D. *et al. Science* **238,** 1386-1392 (1987).
15. Rijsewijk, F. *et al. Cell* **50,** 649-657 (1987).
16. Steward, R. *Science* **238,** 692-694 (1987).
17. Glisin, V., Crkvenjakov, R. & Byus, C. *Biochemistry* **13,** 2633-2638 (1974).
18. van Driel, I. R., Wilks, A. F., Poetersz, G. A. & Goding, J. W. *Proc. natn. Acad. Sci. U.S.A.* **82,** 8619-8623 (1985).
19. Gubler, U. & Hoffman, B. J. *Gene* **25,** 263-269 (1983).
20. Feinberg, A. P. & Vogelstein, B. *Anal. Biochem.* **137,** 266-267 (1984).
21. Vogelstein, B. *et al. Cancer Res.* **47,** 4806-4813 (1987).
22. Henikoff, S. *Gene* **28,** 351-359 (1984).
23. Bartlett, J. A., Gaillard, R. K. & Joklik, W. K. *Biotechniques* **4,** 210 (1986).
24. Tabor, S. & Richardson, C.C. *Proc. natn. Acad. Sci. U.S.A.* **84,** 4767-4771 (1987).
25. Reed, K. C. & Mann, D. A. *Nucleic Acids Res.* **13,** 7207-7221 (1985).
26. Fogh, J. *Natn. Cancer Int. Monograph* **49,** 5-9 (1978).
27. Andrews, P. W. *et al. Lab. Invest.* **50,** 147-162 (1984).
28. Chomczynski, P. & Sacchi, N. *Anal. Biochem.* **162,** 156-159 (1987).
29. Winter, E., Yamamoto, F., Almoguera, C. & Perucho, M. *Proc. natn. Acad. Sci. U.S.A.* **82,** 7575-7579 (1985).

Three-dimensional NMR spectroscopy of a protein in solution

Hartmut Oschkinat*, Christian Griesinger†, Per J. Kraulis*‡, Ole W. Sørensen†, Richard R. Ernst†, Angela M. Gronenborn*‡§ & G. Marius Clore*‡§

* Max-Planck Institut für Biochemie, D-8033 Martinsried bei München, FRG
† Eidgenössische Technische Hochschule, Laboratorium für Physikalische Chemie, CH-8092 Zürich, Switzerland

The geometric information used to solve three-dimensional (3D) structures of proteins by NMR spectroscopy resides in short (<5 Å) interproton-distance data[1,2]. To obtain these distances, the ^1H-NMR spectrum must first be assigned using correlation and nuclear Overhauser effect (NOE) experiments to demonstrate through-bond (scalar) and through-space connectivities, respectively. Because the NOE is proportional to r^{-6}, distance information can then be derived. The increased resolution afforded by extending NMR experiments into a second dimension[3] enables one to detect and interpret effects that would not be possible in one dimension owing to extensive spectral overlap and much reduced information. A number of small protein structures have previously been solved in this way[1,2]. Extending this methodology to larger proteins, however, requires yet an additional improvement in resolution as overlap of cross-peaks in the two-dimensional (2D) NMR spectra present a major barrier to their unambiguous identification. One way of increasing the resolution is to extend the 2D-NMR experiments into a third dimension. We report here the applicability of three-dimensional NMR to macromolecules using the 46-residue protein α1-purothionin as an example.

Three-dimensional (3D) NMR experiments can be conceived by combining two 2D-NMR experiments leaving out the detection period of the first experiment and the preparation period of the second[4]. This is illustrated in a general way in Fig. 1. The location of a peak in 3D space is described by the chemical shifts of three spins, *i*, *j* and *k*. The information contained within a peak depends upon the nature of the experiment. For example,

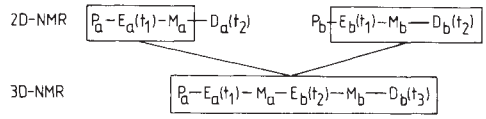

Fig. 1 Generalized representation of 2D- and 3D-NMR experiments. Abbreviations: P, preparations; E, evolution; M, mixing; D, detection.

in a 3D-NMR spectrum combining an NOE experiment with a correlation experiment, the peak at position F1(*i*), F2(*j*), F3(*k*) will arise from through-space coupling between spins *i* and *j* and scalar coupling between spins *j* and *k*.

Although conceptually simple, 3D-NMR has a number of practical problems. Recording a complete 3D-NMR spectrum would be prohibitive in measurement time. For example, a 3D-NMR spectrum with a spectral width of ~8,000 Hz and a resolution of ~10 Hz in each dimension, would require ~1,000 independent increments for the first and second dimensions leading to a total minimum of 10^6 experiments. If typically a four-step phase cycle is necessary, the complete 3D-NMR experiment would take 46 days, assuming a duration of 1 s per

‡ Present addresses: Laboratory of Chemical Physics, Building 2, National Institute of Diabetes and Digestive and Kidney Disorders, National Institutes of Health, Bethesda, Maryland 20892, USA (G.M.C. and A.M.G.); and Department of Molecular Biology, Biomedical Centre, Uppsala University, S-751 Uppsala, Sweden (P.J.K.).
§ To whom correspondence should be addressed.

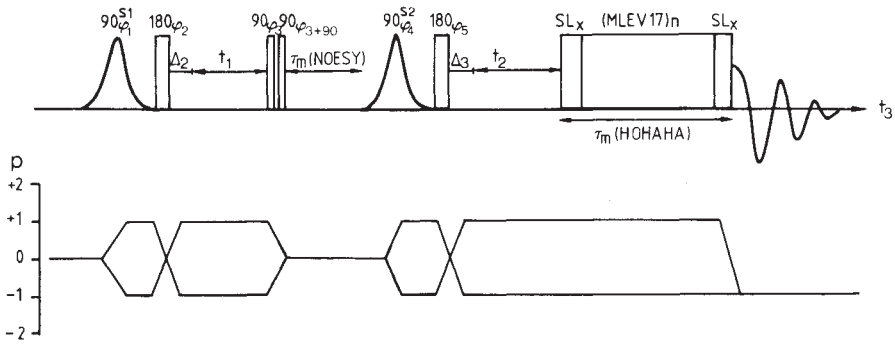

Fig. 2 Pulse sequence used for the 3D-NOESY-HOHAHA spectrum. A minimal 32-step phase cycle was used. This included 180° phase shifts of the two π-pulses to compensate for imperfections and of the semi-selective pulses to remove axial peaks in F1 and F2, and a phase cycle selecting even coherence orders during the mixing process of the NOESY portion of the 3D experiment. A pure phase absorption spectrum was obtained using the time-proportional incrementation method[3] by incrementing the phase of φ_1 and φ_2 and of φ_4 and φ_5 by 90° for every successive t_1 and t_2 value, respectively. The parameters used for the experiment shown in Fig. 2 were as follows: incremental delay (in t_1 and t_2) = 300 μs; 90° pulse (non-selective) = 22.6 μs; 90^{S1}(NH) = 2 ms; $90^{S2}(C^{\alpha}H)$ = 3 ms; SL (trim pulse) = 2 ms; τ_m(NOESY) = 200 ms; τ_m(HOHAHA) = 39 ms; acquisition time = 0.145 s. 64 independent increments were recorded for the F1 and F2 dimensions giving a total of 4,096 increments.

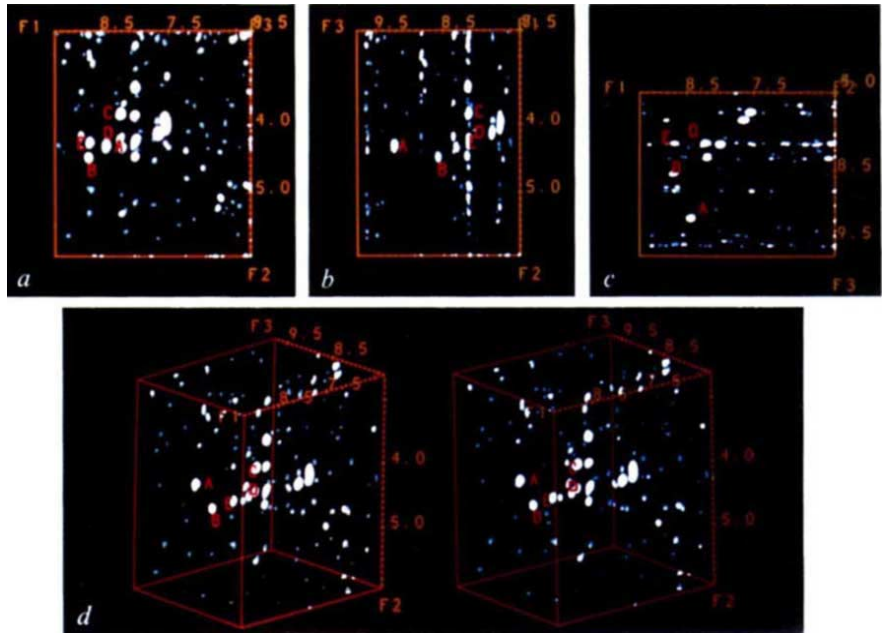

Fig. 3 NH(F1 axis)-C^{α}H(F2 axis)-NH(F3 axis) region of the 500 MHz 3D-NOESY-HOHAHA spectrum of 6.8 mM α1-purothionin in 90% H_2O/10% D_2O at 25 °C. The F1-F2 (*a*), F2-F3 (*b*) and F1-F3 (*c*) projections correspond to 2D NOESY, HOHAHA and relayed NOESY-HOHAHA spectra, respectively. *d*, A stereoview of the 3D spectrum. The assignments of the peaks labelled A to E are as follows: A, Ile_{33}NH(F1)-$Lys_{32}C^{\alpha}$H(F2)-Lys_{32}NH(F3) at 8.56, 4.31, 9.21 p.p.m.; B, Ser_{34}NH(F1)-$Ile_{33}C^{\alpha}$H(F2)-Ile_{33}NH(F3) 8.80, 8.56 p.p.m.; C, Leu_{37}NH(F1)-$Gly_{36}C^{\alpha 1}$H(F2)-Gly_{36}NH(F3) 8.32, 4.19, 8.08 p.p.m.; D, Leu_{37}NH(F1)-$Gly_{36}C^{\alpha 2}$H(F2)-Gly_{36}NH(F3) at 8.32, 3.83, 8.08 p.p.m.; E, Gln_{22}NH(F1)-$Ala_{21}C^{\alpha}$H(F2)-Ala_{21}NH(F3) at 8.80, 4.25, 8.10 p.p.m. (These assignments were derived from the complete assignment given in ref. 13.) The displayed spectrum, which was inspected on an Evans & Sutherland PS390 interactive graphics system using the program FRODO[14], consists of 112(F1) × 129(F2) × 176(F3) real data points with a digital resolution of 13.02 Hz per point in F1 and F2 and of 6.88 Hz per point in F3. The experimental conditions were: 6.8 mM α1-purothionin in 90% H_2O/10% D_2O containing 500 mM sodium phosphate buffer *p*H 4.0. The spectrum was recorded on a Bruker AM500 spectrometer equipped with a selective excitation unit supplemented by a 30 W linear amplifier.

scan. This problem can be eliminated by recording only part of the 3D spectrum (that is, a sub-volume of the total spectrum) using semi-selective excitation pulses[4-6].

For the purposes of illustration, we present a sub-spectrum comprising the NH-C^{α}H region to demonstrate the utility of 3D-NMR in sequential resonance assignment. The general strategy for sequential assignment involves the identification of the following through-space (NOE) and scalar (J) pathways:

$$\mathrm{NH}(i) \xleftrightarrow{\mathrm{NOE}} \mathrm{NH}(i+1) \quad (1)$$

$$\mathrm{NH}(i) \xleftrightarrow{\mathrm{J(+NOE)}} \mathrm{C}^{\alpha}\mathrm{H}(i) \xleftrightarrow{\mathrm{NOE}} \mathrm{NH}(i+1) \quad (2)$$

$$\mathrm{NH}(i) \xleftrightarrow{\text{relayed J (+NOE)}} \mathrm{C}^{\beta}\mathrm{H}(i) \xleftrightarrow{\mathrm{NOE}} \mathrm{NH}(i+1) \quad (3)$$

Through-space connectivities are detected by the NOESY (two-dimensional nuclear Overhauser spectroscopy) experiment[7,8]. Through-bond connectivities can be measured by correlated spectroscopy (COSY[9]) that delivers exclusively direct connectivities. A more versatile approach, however, is total-correlated spectroscopy, known as TOCSY[10] or homonuclear Hartmann-Hahn (HOHAHA)[11] spectroscopy, which detects successively direct, single and multiple relayed scalar connectivities as the mixing time is increased. The 3D-NMR experiment selected for illustration was a NOESY-HOHAHA with detection of inter- and intra-residue NOE connectivities between NH and C^{α}H protons in the first part of the experiment and J-coupling intra-residue connectivities between $C^{\alpha}H(i)$ and $NH(i)$ protons in the second part. This is achieved using semi-selective Gaussian excitation pulses[12] centred in the middle of the NH and C^{α}H regions for the preparation pulse and the last pulse of the mixing process, respectively, in the NOESY part of the sequence. In this way a 3D spectrum is obtained with restricted spectral widths in the F1 and F2 dimensions and the full spectral width in the F3 dimension. The experimental scheme is shown in Fig. 2.

The 3D-NOESY-HOHAHA experiment was recorded in ~69 h at 500 MHz on a 6.8 mM sample of α1-purothionin in 90% H_2O/10% D_2O at 25 °C. Recording the spectrum in H_2O is required to observe the exchangeable NH protons. The suppression of the huge water signal (~100 M) renders the experiment technically demanding. This was achieved by on-resonance irradiation during the relaxation delay and during the NOESY

mixing period. The NOESY and HOHAHA mixing times were 200 ms and 39 ms, respectively.

The results of this experiment are illustrated in Fig. 3. The F1-F2 projection (Fig. 3a) corresponds to a NOESY spectrum of the NH(F1 axis)-$C^{\alpha}H$(F2 axis) region; the F2-F3 projection (Fig. 3*b*) to a HOHAHA spectrum of the $C^{\alpha}H$(F2 axis)-NH(F3 axis) region; and finally the F1-F3 projection (Fig. 3*c*) to a relayed NOESY-HOHAHA spectrum of the NH(F1 axis)-NH(F2 axis) region. A stereoview of the cube is shown in Fig. 3*d*. Two sorts of peaks are present: auto-peaks which arise solely from intra-residue effects, and combined intra- and inter-residue-effect peaks. The former have the chemical shift of the NH(i) proton in the F1 and F3 dimensions and the chemical shift of the $C^{\alpha}H(i)$ proton in the F2 dimension, whereas the latter have the chemical shifts of the NH($i+1$), CαH(i) and NH(i) protons in the F1, F2 and F3 dimensions, respectively. The assignments of five such combined intra- and inter-residue peaks are given in Fig. 3. It will be noted that the strongest peaks of that kind arise from β-strand structures. This is because the contribution from the scalar CαH(i)-NH(i) and NOESY $C^{\alpha}H(i)$-NH($i+1$) interactions are very large in such cases owing to sizeable values for the coupling constant $^{3}J_{HN\alpha}$ and very short $C^{\alpha}H(i)$-NH($i+1$) distances (~2.2 Å), respectively.

Informative 3D-NMR spectra of proteins can be obtained in a reasonable time with concentrations of material no higher than those regularly used in 2D-NMR experiments. What do such 3D-NMR experiments offer? In the case presented here they provided separation of $C^{\alpha}H(i)$-NH($i+1$) inter-residue NOEs in a third dimension according to the chemical shift of the NH proton of residue i, thereby permitting us to identify a number of inter-residue effects that could not be assigned by 2D-NMR owing to overlap with intra-residue $C^{\alpha}H(i)$-NH(i) cross-peaks. For example, in the 2D-NOESY experiments, the $C^{\alpha}H(i)$-NH($i+1$) cross peaks between Ala 21 and Gln 22 (4.25, 8.80 p.p.m.), Ile 33 and Ser 34 (4.46, 8.80 p.p.m.), and Gly 36 ($C^{\alpha 1}H$) and Leu 37 (4.19, 8.32 p.p.m.) are superimposed on the intra-residue $C^{\alpha}H(i)$-NH(i) cross-peaks of Asn 14 (4.22, 8.80 p.p.m.), Ser 35 (4.48, 8.81 p.p.m.) and Leu 37 (4.20, 8.32 p.p.m.), respectively[13]. In the 3D-NOESY-HOHAHA spectrum, however, the chemical shifts of these two sets of peaks differ in the F3 dimension. Thus the inter-residue cross-peaks in the 2D-NOESY spectrum give rise to mixed inter- and intra-residue cross-peaks in the 3D-NOESY-HOHAHA spectrum (Fig. 3) with NH proton chemical shifts of Ala 21 (8.10 p.p.m.; peak E), Ile 33 (8.56 p.p.m.; peak B) and Gly 36 (8.08 p.p.m.; peak D), respectively, in the F3 dimension, which differ from those of the auto-peaks of Asn 14 (8.80 p.p.m.), Ser 35 (8.81 p.p.m.) and Leu 37 (8.32 p.p.m.), respectively.

Many further useful 3D-NMR experiments can be envisaged. A particularly useful, although technically difficult, 3D-NMR experiment seems to be a HOHAHA-NOESY performed in H_2O with $C^{\alpha}H$ and NH protons in the F1 and F2 dimensions, respectively, which would provide the crucial NH-aliphatic proton NOEs. Other potentially useful experiments would include the combination of the NOESY experiment with a heteronuclear correlation experiment; two such experiments would be to spread the NH-aliphatic and C^{α}-NH/aliphatic NOEs in a third dimension according to the ^{15}N and ^{13}C chemical shift, respectively, of the directly bonded heavy atom.

This work was supported by the Max-Planck Gesellschaft and the Bundesministerium für Forschung und Technologie (G.M.C. and A.M.G.). P.J.K. is supported by the Swedish Natural Science Research Council. We thank Alwyn Jones for helpful discussions concerning the displaying of 3D-NMR spectra.

Received 14 December 1987; accepted 3 February 1988.

1. Wüthrich, K. *NMR of Proteins* (Wiley, New York, 1986).
2. Clore, G. M. & Gronenborn, A. M. *Protein Engineering* **1**, 275-288 (1987).
3. Ernst, R. R., Bodenhausen, G. & Wokaun, A. *Principles of Nuclear Magnetic Resonance in One and Two Dimensions* (Clarendon, Oxford, 1987).
4. Griesinger, C., Sørensen, O. W. & Ernst, R. R. *J. magn. Reson.* **73**, 574-579 (1987).
5. Griesinger, C., Sørensen, O. W. & Ernst, R. R. *J. Am. chem. Soc.* **109**, 7227-7228 (1987).
6. Brauschweiler, R., Madsen, J. C., Griesinger, C., Sørensen, O. W. & Ernst, R. R. *J. magn. Reson.* **73**, 380-385 (1987).
7. Jeener, J., Meier, B. H., Bachmann, P. & Ernst, R. R. *J. chem. Phys.* **71**, 4546-4553 (1979).
8. Anil Kumar, Ernst, R. R. & Wüthrich, K. *Biochem. biophys. Res. Commun.* **95**, 1-6 (1980).
9. Aue, W. P., Bartholdi, E. & Ernst, R. R. *J. chem. Phys.* **64**, 2229-2246 (1976).
10. Braunschweiler, L. & Ernst, R. R. *J. magn. Reson.* **53**, 521-528 (1983).
11. Davis, D. G. & Bax, A. J. *Am. chem. Soc.* **107**, 2821-2822 (1985).
12. Bauer, C., Freeman, R., Frenkiel, T., Keeler, J. & Shaka, A. J. *J. magn. Reson.* **58**, 442-457 (1984).
13. Clore, G. M. *et al. J. molec. Biol.* **193**, 571-578 (1987).
14. Jones, T. A. *J. appl. Crystallogr.* **11**, 268-272 (1978).

Heparan sulphate bound growth factors: a mechanism for stromal cell mediated haemopoiesis

R. Roberts, J. Gallagher*, E. Spooncer, T. D. Allen, F. Bloomfield & T. M. Dexter

Departments of Experimental Haematology and *Medical Oncology, Paterson Institute for Cancer Research, Christie Hospital and Holt Radium Institute, Withington, Manchester M20 9BX, UK

The proliferation and development of haemopoietic stem cells takes place in close association with marrow stromal cells[1,2]. This intimate cell contact presumably enables the stem cells and their progeny to respond to stimuli present on the stromal cell surface. While the nature of these stimuli has not been determined, it is likely that growth factors play some role. Recently, it was demonstrated that the natural and the recombinant haemopoietic growth factor, granulocyte/macrophage colony stimulating factor (GM-CSF), could be adsorbed out of solution by an extract of human marrow stromal extracellular matrix (ECM) with retention of biological activity[3]. However, the precise ECM molecules involved were not identified. Here, we clearly demonstrate that the major sulphated glycosaminoglycan of mouse marrow stroma, heparan sulphate[4], possesses the ability to adsorb both GM-CSF and the multilineage haemopoietic growth factor, Interleukin 3 (IL-3). Furthermore, these growth factors, once bound, can be presented in the biologically active form to haemopoietic cells.

In these experiments, we used two growth-factor-dependent multipotent cell lines: FDCP-Mix A4 which responds to IL-3 and FDCP-Mix A_7 which responds to both to IL-3 and GM-CSF[5]. To examine the role that glycosylation of growth factors plays in the ability to bind to components of the ECM, both native 'n' (glycosylated) and *Escherichia coli*-derived recombinant 'r' (non-glycosylated) IL-3 and GM-CSF were used. Initially, we examined the ability of a commercially available ECM preparation (Matrigel) to bind and present these growth factors. The data (Fig. 1*a* and *b*) clearly show that when FDCP-Mix A4 and FDCP-Mix A_7 are added to Matrigel which has been pre-incubated with IL-3 or GM-CSF, they can survive and proliferate.

We could exclude the possibility that cell survival occurred in response to growth factor released by diffusion from Matrigel because the overlying medium from growth-factor-treated Matrigel plates was unable to support the growth of IL-3 or GM-CSF-dependent cells. We conclude, therefore, that the stimulus for growth is *bound* growth factor. Significantly, both native and recombinant growth factor could support the growth of the stem cells, indicating that the protein portion of the growth factor is responsible for binding. It is also clear the the bound growth factors continue to express functional domains for interaction with receptors on the target cells.

We investigated whether enzymatic digestion of the glycosaminoglycan components of the Matrigel had an effect on the ability of the ECM to bind and present growth factors. Two enzymes with differing specificities were used: heparitinase, which digests heparan sulphate and chondroitinase ABC, which digests chondroitin sulphate. The data (Fig. 2*a* and *b*) show